Combined correction with regression for measured respiratory, cardiac, and capnometry variations in pain FMRI studies improves model fit

K. M. Vogt[1], J. W. Ibinson[1,2], R. H. Small[3], and P. Schmalbrock[4]

[1]Biomedical Engineering, The Ohio State University, Columbus, Ohio, United States, [2]Anesthesiology, University of Pittsburgh Medical Center, Pittsburgh, Pennsylvania, United States, [3]Anesthesiology, The Ohio State University, Columbus, Ohio, United States, [4]Radiology, The Ohio State University, Columbus, Ohio, United States

Introduction: Functional magnetic resonance imaging (FMRI) experiments employing pain stimulation are particularly contaminated with physiologic noise, as many cardiopulmonary parameters change significantly in response to pain. These include increased respiratory rate and tidal volume and decreased end-tidal carbon dioxide ($ETCO_2$) concentration, heart rate, and cerebral blood flow [1]. Slice-by-slice linear regression-based correction schemes for pain FMRI using measured respiratory [2] and cardiac [3] fluctuations improve model fit, eliminate false activations, and allow detection of true activations previously masked by physiologic noise. Unlike modeling techniques commonly used for physiologic noise correction [4], the correction method used in this study makes no assumptions about the temporal characteristics of physiologic noise. Rather, data collected from respiratory, cardiac, and $ETCO_2$ monitoring are regressed against the MR data, which is only corrected where a significant correlation is detected between the physiologic and functional data time-series. The effects of combining different physiologic corrections in this manner are assessed.

Methods: Seven subjects (4 male, aged 27 – 46, mean = 31 ± 6) participated in a painful transcutaneous electrical nerve stimulation FMRI study. Block stimulus design was used with four 30s pain epochs. Images were collected on a 1.5 T General Electric scanner (GRE EPI, TR=3s, TE=50ms, 90º flip, 64x64 matrix, in-plane resolution=3.75 x 3.75mm, 28 slices, 5mm axial gave full-brain coverage). Images were pre-processed with FSL's FEAT v5.4 before physiologic correction. During scanning pulse plethysmograph (PPG), respiratory depth, measured with a respiratory belt (RB) strain gauge, and expired carbon dioxide concentration were measured in real-time and recorded continuously (200 Hz sampling). Based on the recorded timing of slice acquisition relative to the peaks of the PPG, unit cycle PPG values were determined for each slice, as in RETROICOR [4]. Respiratory belt data were not further processed and the amplitude value for each slice was used directly. Both RB and PPG data were individually regressed against each voxel timecourse independently and significantly correlated ($p<0.05$) signal variances were subtracted from the data. The expired CO2 waveforms were processed to find the end-tidal value that corresponded to each acquisition volume and these values were used directly in the GLM. Functional activation maps were determined with FEAT and adjusted coefficient of determination (R_a^2) values were calculated for each voxel time-series as in [5]. Mean R_a^2 values are averaged across all voxels in the brain. The effects of inclusion of each physiologic parameter in the model on activated voxels and R_a^2 were examined individually and for all possible combinations of the three corrections.

Results: The distribution of contaminated voxels is consistent with previous reports; cardiac noise is localized to the brain vasculature and the effects of respiratory and $ETCO_2$ correction are more diffuse. Changes in one slice of the average activation map with correction are shown in Figure 1. For each different model, the changes in the number of active voxels and the maximum and mean R_a^2 values averaged across all subjects are listed in Table 1 and shown graphically in Figure 2. Taking the row highlighted in green as an example, it is important to note that, with full correction, the <1% net change in voxel count is comprised of gains and losses in activated voxels (see middle-right of the two panels in Figure 1), as both false-positive and false-negative activations are corrected.

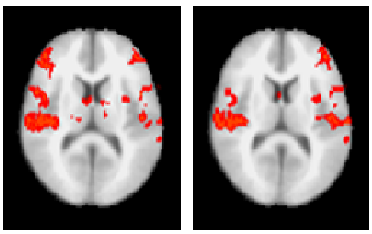

Fig. 1. Group-average activation map for one slice for uncorrected data (left) and with the full correction model (Pain + RB + PPG + $ETCO_2$) applied (right).

Table 1 & Fig. 2. Percent change in R_a^2 and activated voxels with different corrections applied

Noise Parameters in Model	Percent Changes: Max R_a^2	Mean R_a^2	Voxel Count
PPG	13.1	16.1	-3.3
RB	48.3	49.3	-9.9
$ETCO_2$	13.9	68.4	8.7
RB + $ETCO_2$	55.3	113.3	3.8
RB + PPG	57.1	65.0	-18.6
PPG + $ETCO_2$	17.7	84.5	6.1
RB + PPG + $ETCO_2$	62.1	129.1	-0.8

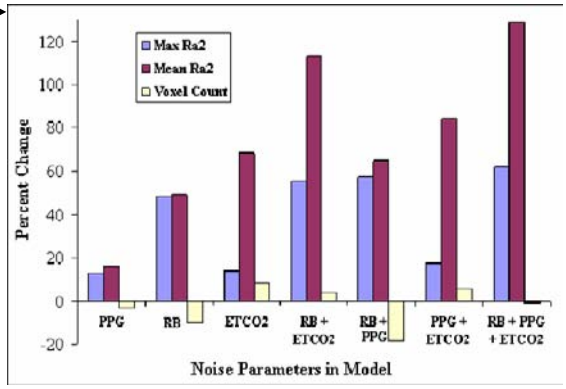

Discussion: Razavi et al. [5] presented using R_a^2 as a measure of FMRI model quality and demonstrated that the inclusion of cardiac and respiratory parameters in the model resulted in improvements indicated by R_a^2 increases. End-tidal $ETCO_2$ predicts arterial CO_2, which is directly related to cerebral blood flow, and $ETCO_2$ fluctuations correlate with significant BOLD signal changes [6]. This current work differs from established FMRI noise correction methods, such as RETROICOR [4] in two important ways: **inclusion of $ETCO_2$ correction**, which improves model fit, and **regression, rather than modelling** of physiologic noise. Regression determines the correlation between physiologic measurements and MR signal and only changes the data at voxels where the correlation surpasses a significance threshold. This method is thus unlikely to induce correlation in or add noise to the data. The improvement of GLM fit with the addition of each physiologic parameter is shown by the consistent increases in R_a^2 shown for each case in Table 1 and Figure 2. These model-fit improvements overshadow the small overall changes in the number of active voxels in the brain. This work also reveals the profound effects of physiologic noise correction on pain FMRI activation maps.

References: [1] Ibinson and Small. *Anesthesiology*, 2004. 101: p. A-1059. [2] Ibinson, et al. *Proc ISMRM*, 2005. 13: p. 1569. [3] Vogt, et al. *Proc ISMRM*, 2006. 14: p 1143. [4] Glover, et al., *MRM*, 2000. 44(1): p.162-7. [5] Razavi, et al. *Hum Brain Mapp*, 2003. 20: p.227-38. [6] Wise, et al. *Neuroimage*, 2004. 21(4): p.1652-64.